^{23}Na and ^{27}Al in β-alumina solid electrolytes

Marco Villa
Istituto di Fisica Generale "A. Volta" e Gruppo Nazionale di Struttura della Materia del Consiglio Nazionale delle Ricerche, Via Bassi 6, 27100 Pavia, Italy

John L. Bjorkstam
Department of Electrical Engineering, University of Washington, Seattle, Washington 98195
(Received 31 August 1979; revised manuscript received 24 June 1980)

In a companion paper, we discussed second-order quadrupolar effects in solids and the theory of the NMR response of a two-dimensional (2D) fluid. This paper illustrates the theoretical treatment through a consideration of the NMR response of ^{23}Na and ^{27}Al in β-alumina. It is shown that dynamical information is contained in the temperature dependence of the second-order quadrupolar shifts. The stationary and fluctuating components of the electric field gradient at the Na^+ position are obtained from quadrupolar shift measurements. Utilizing these parameters in a 2D-continuum diffusion model for Na^+, we are able to account for a number of experimental observations: angular, frequency, and temperature dependence of ^{23}Na transition rates, narrowing of the ^{23}Na satellites, and temperature dependence of the spin-lattice relaxations rates for ^{27}Al. Reasons are given for the success of this model on the NMR time scale.

I. INTRODUCTION

A companion paper,[1] hereafter referred to as I, dealt with some effects of reduced dimensionality upon the motional correlation functions which appear in nuclear magnetic relaxation. It was further shown that second-order quadrupolar contributions to the first moment of a resonance line can give the same dynamical information with respect to atomic motion as does that of spin-lattice relaxation rates. In this article we present experimental verification of considerations developed in I through a study of quadrupolar relaxation effects in the superionic conductor, Na β-alumina. Equations of Paper I will henceforth be referenced as (I-n).

We consider those quantities whose evaluation requires an average over all occupied sites, such as: first moment of a line, spin-lattice transition probabilities, etc. Theoretical expressions for these quantities have been given in I. It should be stressed that the theory of Paper I does not describe phenomena such as the "structure" of a line or any other effect that may be typical of the NMR response of a multiphase system. Therefore, in analyzing the ^{23}Na NMR response of β-alumina, we will generally deemphasize discussion of the temperature region below 140 K at crystal orientations where both central[2] and satellite lines[3] show structure.

In the high-frequency regime (see Paper I), the expected behavior of the spectral densities for diffusion depends strongly upon the model assumed for the motion. In particular, in three dimensions (3D), lattice diffusion (or hopping) models lead to spectral densities which have approximately a Lorentzian shape. Instead, models based upon continuum equations lead to enhanced high-frequency spectral densities with a weaker frequency dependence when compared with Lorentzian densities (see Fig. 1 and Table I in Paper I). These theoretical results were reported as early as 1953. They have been discussed by Torrey in the frame of a classical random-walk formalism.[4] More recently, Hwang and Freed confirmed these facts by giving numerical solutions for particles diffusing according to the Smoluchowski equation.[5] In the last part of this paper we will briefly discuss why the experimental NMR results for β-alumina are better described by a continuum diffusion model than a lattice hopping model.

II. GENERAL INFORMATION AND EXPERIMENTAL

The structural, thermal, spectroscopic, and electrical properties of β-alumina-type compounds have been reviewed several times[6] but are still under active investigation. In the ideal β-alumina crystal, Na^+ lies in a mirror plane between two spinel blocks of aluminum oxide (see Fig. 1). Therefore, the electric field gradient (EFG) at every point in the plane is equivalent to that created by a planar distribution of charges. Thus, the formalism developed in Sec. III of Paper I can be applied.

Pulse and cw NMR experiments were performed on melt-grown crystals supplied by Union Carbide. These crystals contained 22 at.% excess sodium in comparison with the ideal formula $Na_2O \cdot 11Al_2O_3$. No differences in our results have been noticed between samples annealed at 350 °C or left in molten

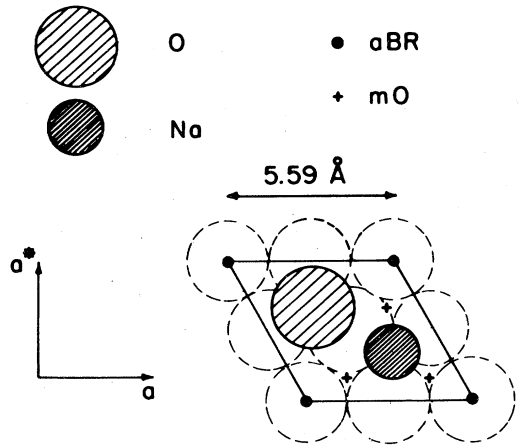

FIG. 1. Atomic arrangement of the mirror plane in Na β-alumina. Dashed circles are the oxygens of the spinel block. Na is shown in a Beevers-Ross (BR) position.

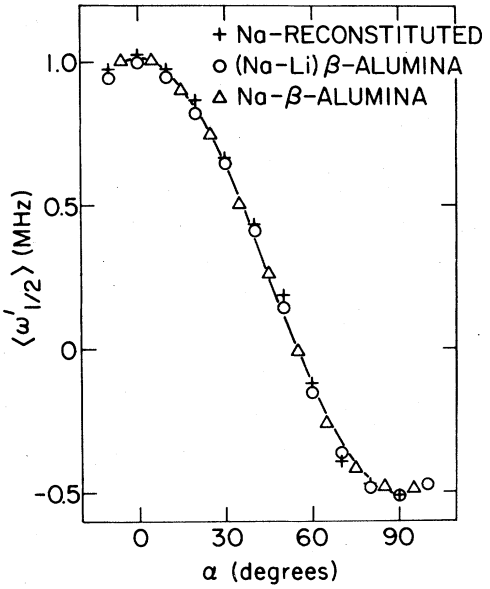

FIG. 2. Displacement of a satellite line of ^{23}Na at RT and 14.2 MHz in various crystal of β-alumina: Na β-alumina (Δ); mixed Na-Li β-alumina ($\sim$ 50 at.% Li substituted) (o); Na β-alumina crystal obtained by exchanging the Ag^+ of Ag β-alumina in molten $NaNO_3 + NaCl$ at $\sim 400\,^{\circ}C$ (+).

$NaNO_3$ for one day, and samples which were exposed for months to the atmosphere. At room temperature (RT), no angular dependence of the ^{23}Na signal for c-axis rotation (i.e., rotation about $c \perp \vec{H}_0$) has been observed. Therefore, Eq. (I-B4) is experimentally justified for ^{23}Na in β-alumina. The crystals were rotated approximately around the a axis, which was kept perpendicular to $\vec{H}_0$. Accuracy of the angular readings was always better than $\pm 2°$. We will first discuss those experiments which give the static parameters $\langle A \rangle$, $\mathfrak{a}(0)$, and $\mathfrak{B}(0)$ defined in I.

III. QUADRUPOLAR SHIFTS

At RT the ^{23}Na satellite lines are very narrow ($\sim$ 10 kHz) and can be easily distinguished from the broad peaks of the ^{27}Al satellites. Shifts of a satellite line from the position occupied by the central line at $\alpha = 0°$ are shown in Fig. 2. These shifts follow well Eq. (I-18) and allow precise evaluation of the constant $c\langle A \rangle = 3.19 \times 10^6$ sec^{-1}. This is a convenient unit of measure for the ^{23}Na quadrupolar interaction and will be designated by κ. As indicated in Fig. 2, the value of κ does not depend upon partial substitution of Na^+ with other cations or the substitutional history of the sample. Moreover it has been found to be nearly temperature independent in the 140–300 K range. Figure 3 shows the absorption derivatives of the central line (to the right) and of the two satellites collapsed into a single line at the magic angle ($\alpha = 54°44'$). The recording was taken at RT and 14.2 MHz. The vertical line indicates the position of ^{23}Na in the absence of quadrupolar effects. Second-order effects are apparent from both the satellite and central line positions. The theoretical position of the lines, as given by the expressions for the shifts in the fast motion limit [see Eq. (I-20) and the correspond-

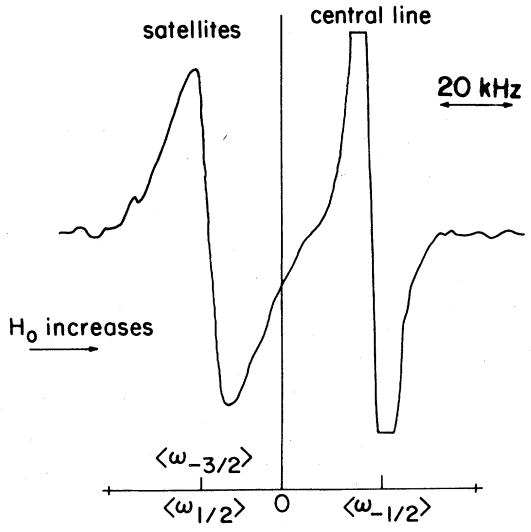

FIG. 3. ^{23}Na absorption derivatives at RT and 14.2 MHz. The magic angle setting for $\alpha(55°44')$ was reached by trial and error. The two collapsed satellites are at the left and are separated from the central line by second-order effects (see text).

ing expression for $\langle\omega_{3/2}\rangle$], are shown at the bottom of Fig. 3. The results confirm that at RT we are approximately in the fast motion regime. This point will be further discussed in connection with the chemical shift of ^{23}Na.

Figure 4 shows shifts (σ) of the ^{23}Na central line at 77 K and 14.2 MHz with respect to the aqueous NaCl signal. As has been reported,[2] at several angles the central line has a well-resolved structure. However, the average shift of the broad resonance should fall between the absolute maximum (σ_+) and the absolute minimum (σ_-) of the absorption derivative. Near $\alpha=0°$ and 90° the lines collapse into a symmetrical line, the position of which can be evaluated with reasonable accuracy as $\langle\omega_{-1/2}\rangle=\frac{1}{2}(\sigma_++\sigma_-)$. From these two shifts one deduces [see Eq. (I-19)]: $c^2\mathcal{A}(0)=0.9\kappa^2$, $c^2\mathcal{B}(0)=0.17\kappa^2$, $\langle\eta(2D)\rangle=0.43$, and the solid line in Fig. 4. Correctness of the angular dependence inferred from the 77 K measurements is confirmed by the data of Boilot *et al.*[7] who, at 100 K, found a single line at all angles. Their shifts, normalized to 14.2 MHz, are shown in Fig. 4. From the fact that $\langle A^2\rangle_{100\,K}<\langle A\rangle^2_{RT}$ it is apparent that some change in the distribution of the EFG's occurs between 100 K and RT. To demonstrate this change, we substitute in Eq. (I-19) the values

$$c^2\mathcal{A}(0)a_s(\omega)\simeq f\kappa^2\omega^{-1}\ ,\qquad c^2\mathcal{B}(0)b_s(\omega)\simeq g\kappa^2\omega^{-1}\ , \tag{1}$$

and calculate the nondimensional quantities f and g from the experimental angular dependence of $\langle\omega_{-1/2}\rangle$. To good approximation, the quantities f and g are proportional, respectively, to $\langle\bar{A}^2\rangle$ and $\langle\bar{B}^2\rangle$ where the temporal averages $(\bar{\ })$ are taken over a time of the order of a Larmor period. Figure 5 reports the temperature-dependent values of f, g, and $\langle\eta(2D)\rangle\equiv(g/f)^{1/2}$ as deduced from the central line quadrupolar shifts at $\alpha=0°$ and 90°. An abrupt change is evident between 100 and 130 K. Above 130 K, f relaxes toward 1 while g and $\langle\eta(2D)\rangle$ relax toward 0, as expected. It can be concluded that different NMR parameters characterize the ^{23}Na resonance above 130 and below 100 K, respectively. For the high-temperature phase, assuming that the f and g values at 130 K are proportional to the square of the EFG fluctuations, we would have

$$c^2\delta\mathcal{A}(0)=0.36\kappa^2\ ,\qquad c^2\mathcal{B}(0)=0.27\kappa^2\ . \tag{2}$$

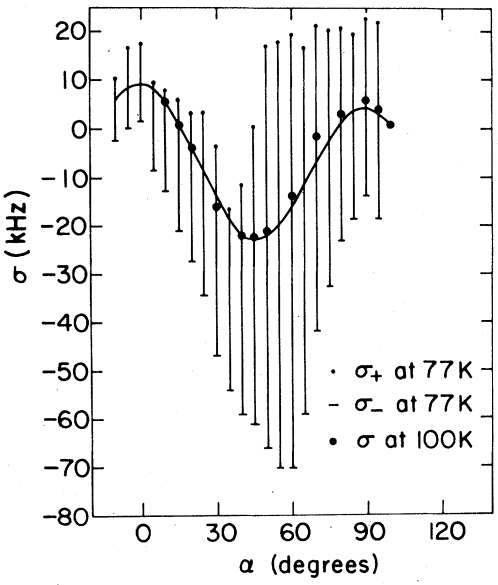

FIG. 4. Angular dependence of the ^{23}Na central line shifts (σ) at 14.2 MHz (see text). The bars connecting σ_+ and σ_- give an approximation of the width of the central lines at 77 K. Filled circles represent data taken from Ref. 7, and the solid line is the theoretical curve.

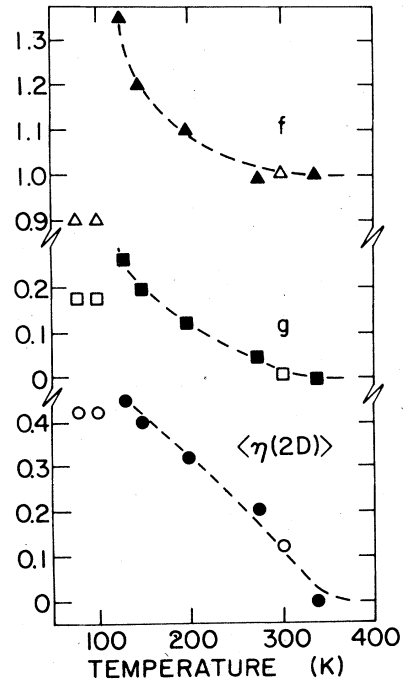

FIG. 5. Behavior of f, g, and $\langle\eta(2D)\rangle$ vs T. Filled symbols represent data extracted from Ref. 8.

IV. SPIN-LATTICE RELAXATION

We will indicate by $M_{1/2}(t)$ the magnetization due to the difference in population between the $m=\pm\frac{1}{2}$ levels and by $M^{eq}_{1/2}$ its value at thermal equilibrium. After a rf pulse has been applied, $M_{1/2}(t)$ relaxes ac-

cording to the equation[9]

$$M_{1/2}^{eq} - M_{1/2}(t) \propto p_1 \exp(-2W_1 t) + p_2 \exp(-2W_2 t) \quad . \tag{3}$$

As long as the 90° or the 180° pulse does not affect the population of the $\frac{3}{2}$ and $-\frac{3}{2}$ levels, it may be shown that $p_1 = p_2$. By using this equality, no complicated fitting procedure is required to extract W_1 and W_2 from the experiment. In the plot of $\ln[M_{1/2}^{eq} - M_{1/2}(t)]$ vs t the slope at the time origin gives $W_1 + W_2$ and the slope at long t is the smaller of $2W_1$ and $2W_2$.

Figure 6 shows the angular dependence of W_1 and W_2 as measured at 21 MHz and RT with the 180° −90° pulse method. The rf field was ~6 G to ensure $p_1 = p_2$ even relatively close to the magic angle where satellites are near the central line. Solid lines represent Eqs. (I-16) and (I-17) where the static parameters are given by Eq. (2) and the reduced correlation functions have been calculated with the 2D-continuum diffusion model (see Sec. IV of I) for $\tau_D = 1.2 \times 10^{-9}$ sec. The values given by the model described in Paper I are

$$\begin{aligned} &\delta a_c(\omega_L) \simeq \tau_D, \quad b_c(\omega_L) \simeq 0.31\tau_D \quad , \\ &\delta a_c(2\omega_L) \simeq 0.68\tau_D, \quad b_c(2\omega_L) \simeq 0.28\tau_D \quad . \end{aligned} \tag{4}$$

W_1 and W_2 have been assigned with the help of the theoretical curves. Considering that τ_D was the only adjustable parameter, the agreement between predictions of the 2D-diffusion model and the experimental relaxation rates is remarkable. However the assignment of W_1 and W_2 for $\alpha = 80°$ and 90° may be open to question. For example, with τ_D values a few times longer than 1.2×10^{-9} sec, the theoretical curves for W_1 and W_2 would not cross above $\alpha = 70°$. However, independent of the model of motion, Fig. 6 confirms that the 2D treatment of I is correct and that $\delta a(t)$ decays more slowly with time than does $b(t)$. In fact, the agreement between calculated and experimental relaxation rates at RT points to the correctness of the theoretical spectral densities of Eq. (4). This equation implies that $\delta a(t)$ has a spectral density higher than $b(t)$ in the low-frequency regime. Moreover, for a Larmor frequency near 20 MHz, $\delta a_c(\omega)$ still shows a marked frequency dependence at RT while for $b_c(\omega)$ one has $b_c(\omega_L) \simeq b_c(2\omega_L)$ [see Eq. (4)].

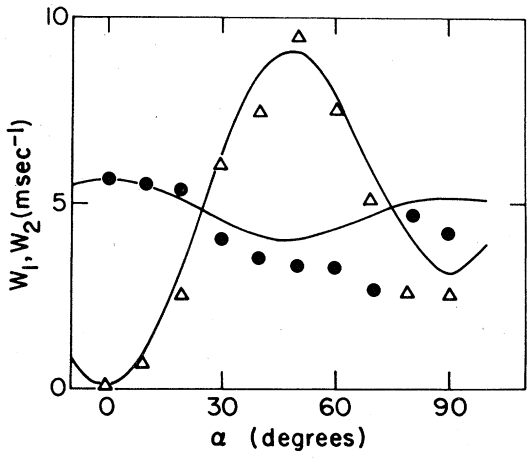

FIG. 6. Angular dependence of the ^{23}Na $W_1(\Delta)$ and $W_2(\bullet)$ at RT and 21 MHz in Na β-alumina.

The temperature and frequency dependence of ^{23}Na spin-lattice relaxation times in melt- and flux-grown crystals of β-alumina have been investigated in some detail by Walstedt *et al.*[10] Here, we compare the Walstedt results for ^{23}Na and our data for ^{27}Al spin-lattice relaxation time T_1^* (Ref. 11) at 21 MHz and $\alpha = 0°$ (see Fig. 7) with the predictions of the 2D-continuum diffusion theory developed in Paper I. In the high-temperature region, the model would predict that activation energies extracted from the relaxation rates are weakly angular dependent and often appreciably smaller than U (see Table I in I). At temperatures below 200 K, the relaxation rates have a small activation energy ($U_{NMR} \simeq 0.033$ eV) and can be described by Eq. (I-26) with $\gamma \simeq 0.23[W(\omega_1)/W(\omega_2) \simeq (\omega_2/\omega_1)^{1.23}]$. Since $U_{NMR}/\gamma \simeq 0.14$ eV, one can conclude that, within experimental error, above 120 K the spin-lattice relaxation mechanism of ^{23}Na is due to a motion having essentially the same activation energy as that for conductivity. The motional diffusion of Na^+ drives also the spin-lattice relaxation process of ^{27}Al. The spin-lattice relaxation time of the ^{27}Al central line for $\alpha = 45°$ at two different frequencies is shown in Fig. 8. At temperatures above the T_1 minimum no frequency dependence is evident and the activation energy is consistent with that observed in diffusion and conductivity measurements. At low temperatures, departure from the ω^2 frequency dependence characteristic of Lorentzian behavior is accompanied by an apparent activation energy differing from that at high temperature. These departures are compatible with Eqs. (I-26) and lead to an activation energy for τ of ~0.16 eV both above and below the T_1 minimum.

As a result of the range of values reported for the conductivity prefactors and activation energies,[6] a comparison between Na^+ conductivity and NMR data can be carried out in a number of ways. If we choose, as before, $\tau_D = 1.2 \times 10^{-9}$ sec at 293 K and an activation energy of $U = 0.164$ eV,[12] the 2D-continuum diffusion model gives, for 21 MHz, the solid curve of Fig. 7. This curve predicts a T_1 minimum near 190 K, in agreement with the ^{27}Al T_1^* results. However, the experimental ^{23}Na T_1 mini-

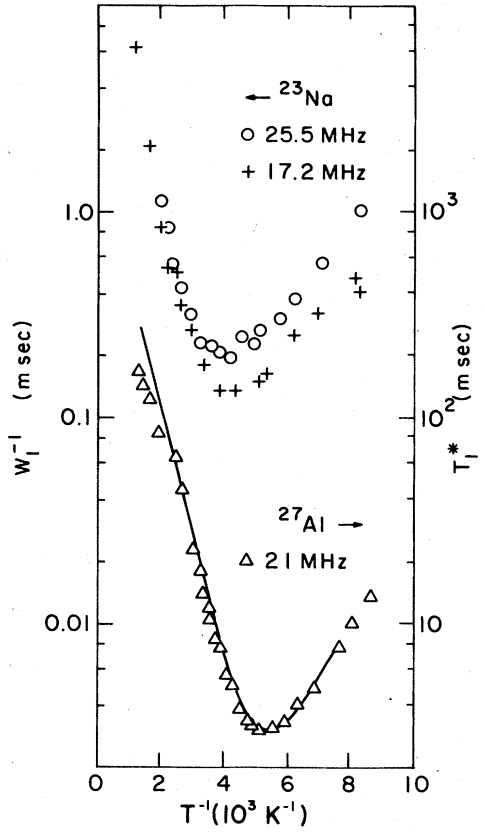

FIG. 7. ^{23}Na relaxation times $(W_1)^{-1}$ vs T^{-1} for the melt-grown crystal of Walstedt *et al.* (Ref. 10) at 25.5 (○) and 17.2 (+) MHz with $\alpha = 45°$ (left vertical scale). ^{27}Al T_1^* in β-alumina (Δ) at 21 MHz and $\alpha = 0°$ (right vertical scale). The solid curve is proportional to the theoretical W_2^{-1} of ^{23}Na calculated with the continuum diffusion model (see text). The single proportionality constant (which simply translates the theoretical curve vertically) has been chosen in such a way as to give a "best fit" to the experimental data.

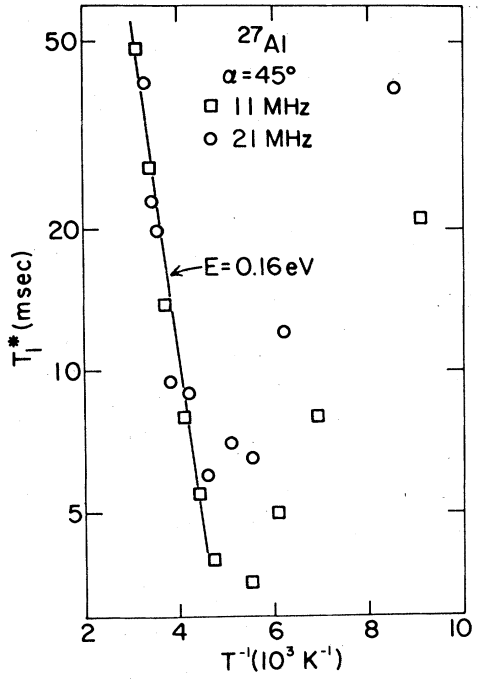

FIG. 8. T_1^* of the ^{27}Al central line at $\alpha = 45°$ and two Larmor frequencies: 21 MHz (○) and 11 MHz (□).

mum at the same frequency occurs near 240 K, indicating that ^{23}Na relaxation occurs through EFG fluctuations with much longer correlation times than for ^{27}Al. In terms of an elementary 2D-continuum diffusion model, which does not include the concepts of individual jump times and jump lengths, NMR measures the time for the nuclei to experience local-field fluctuations responsible for the dominant relaxation process. Assuming that both ^{23}Na and ^{27}Al are relaxed by the same diffusional process, the EFG inhomogeneities must have different characteristic lengths d_0 [see Eq. (I-23)]. These lengths may be estimated from the temperatures ($T_{\min}$) where the T_1 minima occur. Notice that, for the model discussed in Sec. IV of Paper I, the maximum value for the spectral densities occurs at $\omega\tau_D \simeq 10$, so that

$$d_0 \simeq \left[10 D_0 \exp\left(-\frac{U}{kT_{\min}}\right)\omega_L^{-1}\right]^{1/2} .$$

With the D_0 and U values of Whittingam and Huggins[12] we have $d_0^{(Al)} \simeq 3.6$ Å and $d_0^{(Na)} \simeq 10$ Å. Instead, with the diffusion coefficients extrapolated from the conductivity data of Hooper above RT,[13] we obtain $d_0^{(Al)} \simeq 8.5$ Å and $d_0^{(Na)} \simeq 20$ Å. Within the wide limits of the experimental uncertainty, $d_0^{(Al)}$ is equal to a lattice spacing (5.7 Å) while $d_0^{(Na)}$ is 2–3 times such a spacing. It is reasonable to suppose that Na^+ motion over a unit cell would most effectively deform the spinel block in which the ^{27}Al resides. On the other hand, the ^{23}Na T_1 minimum near 240 K results from EFG fluctuations caused by the compensating O^{2-} ions. The distance $d_0^{(Na)}$ is in agreement with the known concentration of these ions. In the Conclusion, we will discuss the compatibility between our interpretation of the NMR data and other experimental results.

V. TEMPERATURE DEPENDENCE OF THE SATELLITE LINEWIDTH

Figure 9 shows the dependence upon temperature of the peak-to-peak (Δ_{pp}) separation of the absorp-

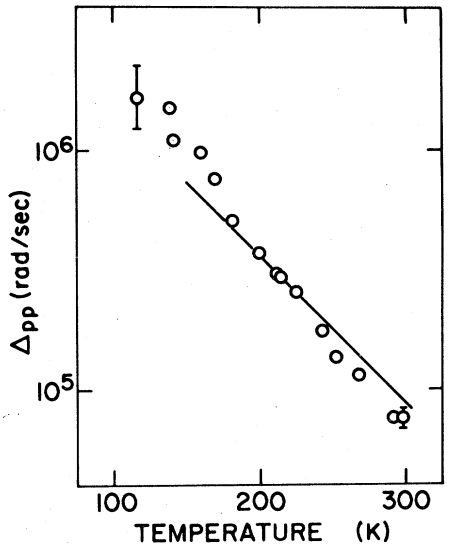

FIG. 9. Peak-to-peak separation of the downfield ^{23}Na satellite line at $\alpha = 0°$. Solid curve gives the theoretical behavior.

tion line derivative for the down-field satellite line at $\alpha = 0°$. The adiabatic contribution to this line has a very simple form since second-order quadrupolar effects are absent. The nonadiabatic contribution, which can be easily estimated, is responsible for less than one-tenth of the RT linewidth (much less below RT). Therefore, the function $R_{1/2}(t)$ for the satellite line at $\alpha = 0°$ can be written [see Eqs. (I-11) and (I-12)]

$$R_{1/2}(t) = \left\langle \exp\left[i \int_0^t dt' \delta\omega_{1/2}(t') \right] \right\rangle \simeq \exp\left[-4c^2 \delta\mathfrak{A}(0) \int_0^t d\tau (t-\tau) \delta a(\tau) \right] . \tag{5}$$

For the case of "fast" motion we can put

$$\int_0^t d\tau (t-\tau)\delta a(\tau) \simeq t \int_0^t d\tau \delta a(\tau) \simeq t \delta a_c(\omega_{\text{local}}) . \tag{6}$$

Then, assuming that the line is Lorentzian ($\Delta_{pp} = 1.15/T_2$), we have

$$\Delta_{pp} \simeq (1.15) 4c^2 \delta\mathfrak{A}(0) \delta a_c(\omega_{\text{local}}) . \tag{7}$$

The solid line in Fig. 9 represents Eq. (7) with $\delta a_c(\omega)$ calculated using the same choice of correlation times as before ($\tau_D = 1.2 \times 10^{-9}$ sec at RT and $U = 0.164$ eV) and a value for the cutoff frequency $\omega_{\text{local}} = 10^7$ sec^{-1}. This cutoff is simply the rounded-off frequency shift of the satellite line at $\alpha = 0°$ (6.3×10^6 sec^{-1}).

VI. NARROWING OF THE CENTRAL LINE

As long as the central line and the satellites are well separated, the nonadiabatic contribution to their widths for spin $I = \frac{3}{2}$, is $W_1 + W_2$. As indicated in Sec. II of Paper I, the secular contribution to the central linewidth is not described by a simple expression in the fast-motion regime. With $\omega_L \tau_D < 1$, study of the central linewidth of ^{23}Na is not necessary in β-alumina since information on $\delta\mathfrak{A}(t)$ and $\mathfrak{B}(t)$ can be obtained in a variety of more simple ways. However, we will present some experiments on the field and angular dependence of the ^{23}Na central line at RT. We anticipate that they will find an explanation and that they will be of some help in the study of quadrupole-perturbed spin systems in cases where dynamical information must be extracted from the central linewidth. At a Larmor frequency of 21 MHz, and at all angles, the free precession signal of the ^{23}Na central line is exponential over more than a decade. The experimental linewidth $\Delta \equiv T_2^{-1}$ is compared with its nonsecular contribution in Fig. 10. In contrast to what has been stated in the literature,[14] even at RT nonsecular effects are unable to account for the entire linewidth, though they seem primarily responsible for its angular dependence. Figure 11 reports the field dependence of Δ from $\simeq 65$ to 3 kG for three different orientations, together with the theoretical behavior of the nonadiabatic contribution (solid lines) as predicted by the continuum diffusion model, with the previously used choice of parameters. The general treatment of Paper I predicts that the adiabatic contribution decreases with increasing

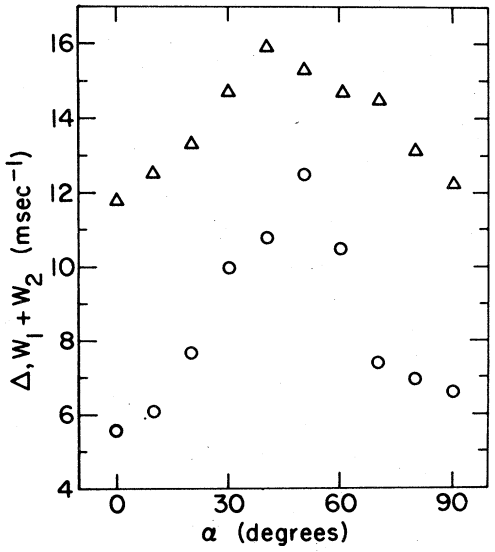

FIG. 10. Total linewidth (Δ) and nonadiabatic contribution to the linewidth $W_1 + W_2$(○) for the ^{23}Na central lines at RT and 21 MHz.

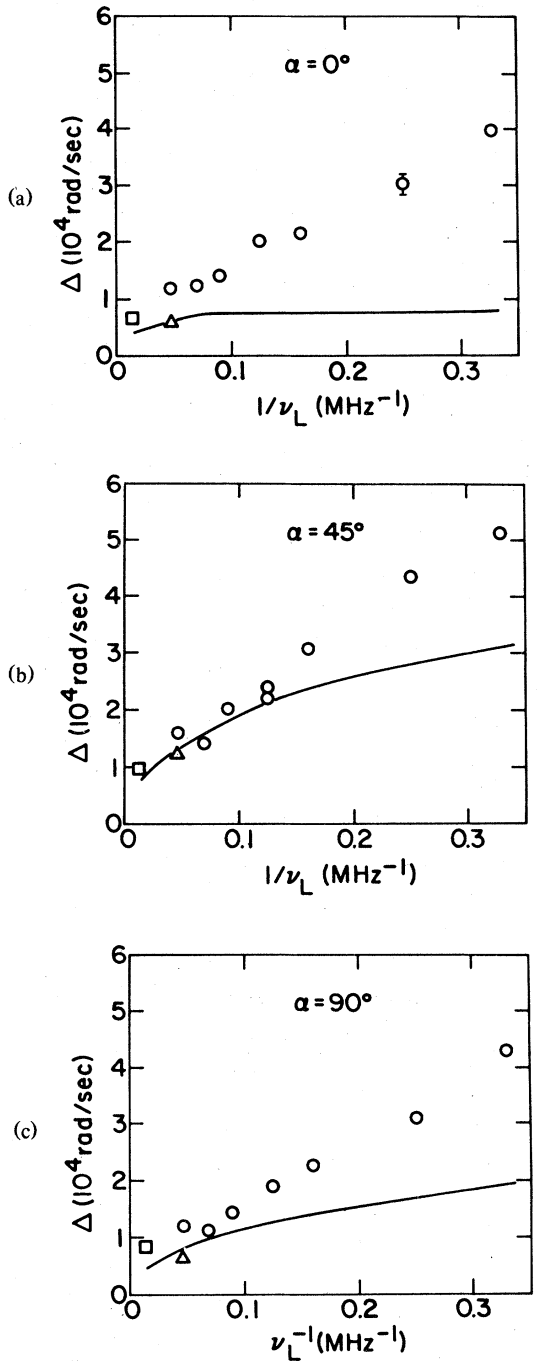

FIG. 11. ^{23}Na central transition linewidth (O) at RT as a function of the Larmor period (ν_L^{-1}) for three different orientations: (a) $\alpha = 0°$; (b) $\alpha = 45°$; and (c) $\alpha = 90°$. Solid lines represent the theoretical nonadiabatic contribution. The values of $W_1 + W_2$ at 21 MHz are represented by triangles. The squares are the T_2 data of West *et al.* (Ref. 2).

temperature and frequency but does not allow a quantitative comparison to be made with the data of Fig. 11. Intuitively, the adiabatic contribution to Δ is proportional to the second moment of a motionally narrowed line, i.e., to ω_L^{-2} in our case. On the other hand, with increasing frequency, effects of atomic motion become less important since it is the averaging which takes place over a time comparable with the Larmor period which decreases the second-order quadrupolar interaction. Whether the field dependence of the adiabatic contribution displayed in Fig. 11 (which is neither linear nor quadratic in ω_L^{-1}) is a general feature of the second-order narrowing process remains to be demonstrated.

VII. CHEMICAL SHIFT OF ^{23}Na

The general expression for the quadrupolar shift of the central line at $\alpha = 0°$ [see Eq. (I-19)] reduces to

$$\langle \omega_{-1/2} \rangle = 6c^2 \mathfrak{B}(0) b_s(2\omega_L) \quad . \tag{8}$$

By putting

$$b_s(\omega) = \omega/(\tau_D^{-2} + \omega^2) \tag{9}$$

and $c^2\mathfrak{B}(0) = 0.27\kappa^2$ [see Eq. (2)], in the low-frequency regime we then obtain

$$\langle \omega_{-1/2} \rangle = 3.3 \times 10^{13} \tau_D^2 \omega_L \text{ sec}^{-1} \quad . \tag{10}$$

On the other hand, the low-frequency regime contribution to the shift of the B part has an angular dependence of the form [see Eq. (I-19)]

$$\langle \omega_{-1/2} \rangle_{B\,\text{part}} \propto (1 - 1.15 \sin^2\alpha) \quad . \tag{11}$$

According to Eq. (10), and assuming $\tau_D = 1.2 \times 10^{-9}$ sec, at RT, there would be a shift of 47 ppm which is of quadrupolar origin. This must be considered when evaluating the chemical shift. It is thus imperative to determine the real chemical shift of ^{23}Na at temperatures above RT since $\langle \omega_{-1/2} \rangle$ for $\alpha = 0°$ goes rapidly to zero with increasing temperature. As a matter of fact, we were not able to measure any further change above 370 K where the shift from our reference (saturated solution of NaCl in water at RT) was 21 ± 5 ppm. Figure 12 gives evidence of the fact that, though small, the effects of the fluctuating components of the EFG are observable at RT. It represents (upper part) the angular dependence of the experimental shifts, with the high-temperature, $\alpha = 0°$, position of ^{23}Na in β-alumina as the reference. The solid curve is the theoretical expression for $\langle \omega_{-1/2} \rangle$ in the high-temperature limit [see Eq. (I-20)]. The lower part shows the difference between data points and solid curve. Both the angular dependence and the absolute values of these differences are approximately described through Eqs. (10) and (11) (solid curve in

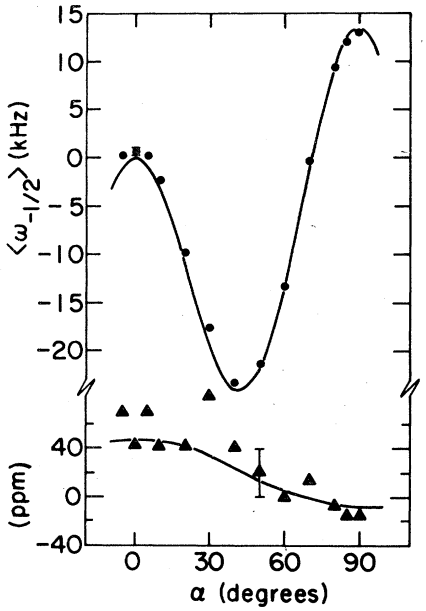

FIG. 12. First moment of the ^{23}Na central line $\langle\omega_{-1/2}\rangle$ vs α at RT and 14.2 MHz. The reference was the position of the ^{23}Na central line at $\alpha = 0°$ and 410 K. The lower part of the figure gives the difference in parts per million (ppm) between the experimental first moment (●) and the theoretical value in the fast-motion limit (upper solid curve). The lower solid curve has been drawn according to Eqs. (10) and (11).

the lower part of the figure). Therefore, as was the case with West *et al.*,[2] the experimental results do not allow determination of an anisotropy in the chemical shift of Na^+ in β-alumina. Instead, a definite anisotropy of the chemical shift is observable in resonances of ^{203}Tl and ^{205}Tl in a partly substituted (~ 60 at.%) single crystal of β-alumina. When a saturated aqueous solution of $TlNO_3$ at RT is taken as the reference, the ^{203}Tl and ^{205}Tl chemical shifts in β-alumina follow well the expression

$$\sigma = (M + N \sin^2\alpha)$$

with $M = -140$ ppm and $N = 175$ ppm.

Since Tl^+ is expected to have chemical shifts at least two orders of magnitude larger than Na^+,[15] we can conclude that the chemical-shift anisotropy of ^{23}Na may be studied only with a resolution better than 1 ppm.

VIII. CONCLUSIONS

The primary purpose of this article was to illustrate the major points of the formal developments of Paper I, i.e., the fact that dynamical information is contained in second-order quadrupolar shifts, and that NMR problems in 3D and 2D require different correlation functions. Attention has already been called to the fact that Lorentzian NMR spectral densities lead to underestimates of the attempt frequency of Na^+ in β-alumina due to the presence of a low-dimensionality effect.[16] There is evidence for such effects in the dispersion which exists even at temperatures above the T_1 minimum. For example, at RT, and 21 MHz the angular dependence of the spin-lattice relaxation rates can be fitted by taking $c^2\delta\mathfrak{A}(0)\delta a_c(\omega_L) = 4.4 \times 10^3$ sec^{-1} while the satellite linewidth at $\alpha = 0°$ requires $c^2\delta\mathfrak{A}(0)\delta a_c(\omega_{\text{local}}) = 1.5 \times 10^4$ sec^{-1}. Thus, even well above the temperature of the T_1 minimum the spectral density $\delta a_c(\omega)$ still increases by more than a factor of three when ω goes from $\omega_L = 1.32 \times 10^8$ sec^{-1} to $\omega_{\text{local}} \simeq 10^7$ sec^{-1}. Directly related to the presence of a low-frequency dispersion in $\delta a_c(\omega)$ is the fact that the Arrhenius plots of relaxation rates and satellite linewidth, for $T > 250$ K, yield an activation energy ($U_{\text{NMR}} \simeq 0.1$ eV) appreciably smaller than that for Na^+ diffusion.

At high temperatures where the correlation times are expected to be short compared with NMR sampling times it is not surprising that a continuum diffusion model gives a quantitatively accurate description of ^{23}Na and ^{27}Al relaxation rates. The interesting point is that this model is able to account for temperature and frequency dependence of T_1 in the low-temperature region. We thus present some qualitative considerations with respect to the limit of applicability of the continuum diffusion model. For 2D systems, we define the mean translational displacement in the time ω_L^{-1} as $l = (4D\omega_L^{-1})^{1/2}$. As long as l is much longer than the step length d_j, continuum diffusion and hopping models give essentially the same results.[4] A minimum in the spin-lattice relaxation times is expected to occur when l becomes of the order of d_0 (minimum approach between spins when dipole-dipole relaxation is considered, or range of the defect for defect diffusion).[17] In our case, d_0 is a parameter measuring the range of the interaction creating the local-field fluctuations responsible for relaxation. If these fluctuations are a result of individual jumps, $d_0 \sim d_j$. This would imply that the continuum diffusion model can be effectively applied only above the temperature of the T_1 minimum and that, below this temperature, T_1 should display the ω_L^{-2} dependence predicted by all hopping models in the high-frequency regime. However, when d_j is small compared to d_0, as is usually the case for liquids, the spin-lattice relaxation rates below the temperature of the minimum can display the $\omega_L^{-3/2}$ dependence typical of continuum diffusion[18] (see Table I in I). In these cases we expect that the distribution of the mobile ions is better described in terms of extended regions over which the probability of finding the ion is nearly constant rather than in terms of occupancy of well localized lattice sites. There is a

similarity between such a distribution and that hypothesized by the "excluded-volume theory" to interpret neutron-diffraction data in α-AgI.[19] However, liquidlike models of motion are not applicable to all superionic compounds. For instance, the ^{19}F relaxation rates in BaF_2 are well described with Lorentzian spectral densities over the entire frequency and temperature range investigated.[20] This is related to the mechanism of diffusion by short-lived Frenkel pairs typical of fluorites. The local field at a ^{19}F position changes every time that a defect "encounters" the neighborhood of the nucleus. The effect of a single encounter upon the local fields is almost equivalent to the effect of a jump of fluorine to an infinite distance since the many, high-frequency jumps during an encounter produce a local field almost uncorrelated with that existing at the beginning. Torrey has shown[4] that the dipolar spectral density for diffusion becomes Lorentzian in the $d_j \to \infty$ limit.

We have now to discuss the consistency between the continuum diffusion interpretation of NMR results in β-alumina and other experimental data. The dynamical picture for Na^+ motion underlying our model is that of a particle which moves between broad and interconnected potential wells by making small, high-frequency jumps. Strong support for this picture comes from recent dynamic simulation experiments in β-alumina by DeLeeuw and Perram.[21] These authors did not find a definite distinction between vibrational and diffusive motion of Na^+ ions for the nonstoichiometric β-alumina. A mechanical simulation experiment of atomic diffusion in a planar lattice by Geisel[22] offers a visual representation of what continuum diffusion may be. For β-alumina, this picture is apparently in contrast with x-ray diffuse scattering results that are interpreted in terms of site-occupancy probabilities.[6] However, it was early noted[23] that a comparison between neutron and x-ray-scattering results at RT indicates the presence of a high-frequency cation motion. In addition, neutron diffraction in the 80–800 K range[24] shows that sodium nuclei are spread over extended regions around the lattice sites. These data agree with the liquidlike features assigned by molecular dynamics[21] to the Na-Na pair-distribution function and indicates that the concept of site occupation has a rather loose meaning in β-aluminas.

Direct measurements of the attempt frequencies for cation motion through optical experiments[6] have also been interpreted as evidence for applicability of a hopping model of motion to β-alumina. Considering the large difference in time scales between NMR and optical experiments, it is not surprising that they are sensitive to different aspects of cation dynamics. Moreover, the cooperative aspects of the Na^+ motion demonstrated by the Wang-Gaffari and Choi electrostatic calculations,[25] requires that the displacement of Na^+ over a lattice spacing is a process accomplished in a sequence of steps. Applicability of continuum diffusion below T_{min} implies the same requirement.

In conclusion, the predictions of a continuum diffusion model with reasonable choices of NMR parameters is in good agreement with ^{23}Na and ^{27}Al NMR data above 140 K. This agreement implies that EFG fluctuations due to localized motions among the *mO*, BR, and *a*BR (BR is Beevers-Ross position) sites occur on a time scale much shorter than that sampled by the NMR. While it may well be that differences in local environments of the cation lead to a distribution of barrier heights,[10] thus making the microscopic interpretation of diffusion a complex percolation problem, for the temperature range discussed here a cation samples all possible local environments in a time needed to move over the distance $d_0^{(Na)}$. Thus the NMR results are insensitive to the distribution of individual barrier heights and lead to the same activation energy as for conductivity in an effective-medium approximation.[26] It should be acknowledged that the approximate and indirect nature of the information on diffusion obtained from ^{23}Na and ^{27}Al NMR does not allow discussion of such a subtle phenomenon as the temperature variation of the Haven ratio.[27,28] In other words, it is not possible to say whether the currently available NMR data should be most appropriately compared with tracer diffusion, or conductivity, results. On the contrary, we believe that ^{27}Al and ^{23}Na NMR data near and below 100 K can be of invaluable help in characterizing the nature of the local motions that appear to be related to the low-temperature glasslike behavior of β-aluminas.[29] Elsewhere,[30] it will be shown that a progressive freezing of these motions can be related to a heat capacity anomaly and to the behavior of the f and g parameters (see Fig. 5) near 100 K.

ACKNOWLEDGMENTS

The financial support of the DOE (Grant No. EY-76-S-06-2225) is gratefully acknowledged. Fondazione Della Riccia (Firenze, Italy) partially supported one of us (M.V.).

[1]J. L. Bjorkstam and M. Villa, Phys. Rev. B 22, 5025 (1980) (preceding paper).
[2]L. C. West, T. Cole, and R. W. Vaughan, J. Chem. Phys. 68, 2710 (1978).
[3]A. Highe, M. Polak, and R. W. Vaughan, in *Fast Ion Transport in Solids, Electrodes and Electrolytes,* edited by P. Vashishta, J. N. Mundy, and G. K. Shenoy (North-Holland, New York, 1979), p. 305.
[4]M. C. Torrey, Phys. Rev. 92, 962 (1953).
[5]L. P. Hwang and J. H. Freed, J. Chem. Phys. 63, 4017 (1975).
[6]J. H. Kennedy, in *Solia Electrolytes,* edited by S. Geller (Springer-Verlag, New York, 1977), p. 105.
[7]J. P. Boilot, L. Zuppiroli, G. Delplanque, and L. Jerome, Philos. Mag. 32, 343 (1975).
[8]C. H. Wei, Ph.D. thesis (University of Washington, 1976) (unpublished).
[9]M. H. Cohen and F. Reif, Solid State Phys. 5, 321 (1957).
[10]R. E. Walstedt, R. Dupree, J. P. Remeika, and A. Rodriques, Phys. Rev. B 15, 3442 (1977).
[11]J. L. Bjorkstam, S. Manzini, and M. Villa, in *Fast ion Transport in Solids, Electrodes and Electrolytes,* edited by P. Vashishta, J. N. Mundy, and G. K. Shenoy (North-Holland, New York, 1979), p. 293.
[12]M. S. Whittingam and R. A. Huggins, J. Chem. Phys. 54, 414 (1971).
[13]A. Hooper, J. Phys. D 10, 1487 (1977).
[14]W. Bailey, S. Glowinkowski, H. Story, and W. L. Roth, J. Chem. Phys. 64, 4126 (1976).
[15]D. E. O'Reilly, in *Nuclear Magnetic Resonance Spectroscopy,* edited by J. W. Emsley, J. Feaney, and L. H. Sutcliffe, (Pergamon, New York, 1966), Vol. 2, p. 1.
[16]P. M. Richards, Solid State Commun. 25, 1019 (1978).
[17]R. Kimmich and G. Voight, Z. Naturforsch. A 33, 1294 (1978).
[18]G. Held and F. Noack, in *Proceedings of the XVIII Congress Ampere, Nottingham, 1974,* edited by P. S. Allen, E. R. Andrew, and C. A. Bates (University of Nottingham Press, United Kingdom, 1975), p. 461.
[19]J. B. Boyce and T. M. Hayes, in *Physics of Superionic Conductors,* edited by M. B. Salamon (Springer-Verlag, Berlin, 1979), p. 4.
[20]D. R. Figueroa, J. H. Strange, and D. Wolf, Phys. Rev. B 19, 148 (1979).
[21]S. W. DeLeeuw and J. W. Perram, in *Fast Ion Transport in Solids, Electrodes and Electrolytes,* edited by P. Vashishta, J. N. Mundy, and G. K. Shenoy (North-Holland, New York, 1979), p. 345.
[22]T. Geisel, in *Physics of Superionic Conductors,* edited by M. B. Salamon (Springer-Verlag, Berlin, 1979), p. 201.
[23]S. M. Shapiro, in *Superionic Conductors,* edited by G. D. Mahan and W. L. Roth (Plenum, New York, 1976), p. 261.
[24]F. Reidinger, Ph.D. thesis, (SUNY-Albany, Albany, 1979) (unpublished).
[25]J. C. Wang, M. Gaffari, and Sang-il Choi, J. Chem. Phys. 63, 772 (1975).
[26]J. Bernasconi, Phys. Rev. B 7, 2252 (1973).
[27]J. N. Mundy, in *Fast Ion Transport in Solids, Electrodes and Electrolytes,* edited by P. Vashishta, J. N. Mundy, and G. K. Shenoy (North-Holland, New York, 1979), p. 159.
[28]H. Sato and R. Kikuchi, in *Fast Ion Transport in Solids, Electrodes and Electrolytes,* edited by P. Vashishta, J. N. Mundy, and G. K. Shenoy (North-Holland, New York, 1979), p. 337.
[29]A. C. Anderson, in *Fast Ion Transport in Solids, Electrodes and Electrolytes,* edited by P. Vashishta, J. N. Mundy, and G. K. Shenoy (North-Holland, New York, 1979), p. 255.
[30]J. L. Bjorkstam, P. Ferloni, and M. Villa, J. Chem. Phys. (in press).